Environ Geol (2009) 58:1703–1711
DOI 10.1007/s00254-008-1670-9

ORIGINAL ARTICLE

Palaeoenvironment of mid- to late Holocene loess deposit of the southern margin of the Tarim Basin, NW China

Tang Zihua · Mu Guijin · Chen Dongmei

Received: 17 May 2008 / Accepted: 25 November 2008 / Published online: 7 January 2009

Abstract Holocene environmental history in the Tarim Basin and the Taklimakan Desert is known mainly from isolated eolian and lacustrine deposits and remain puzzling. Here we present an adequately preserved loess section, covering the past 5000 years, at a highland (2,850 m a.s.l) on the northern slope of Kunlun Mountains. Pollen preserved in the section reveal a drying trend with significant moisture fluctuations around 3000–2600 cal yr BP and 1800 cal yr BP at the study site. Comparing the pollen, grain size from the same section provides a different scene occurred in the Tarim basin and the Taklimakan desert. Comparison of grain size to A/C ration of pollen suggests that active sand southward shifting in south margin of the desert is coincident with increasing moisture condition at the section locality, implying a casual link. This moisture pattern occurred at the upper and lower elevation of the slope is best explained by the vertical variation of local precipitation along the slope.

Keywords Loess · Environmental changes · Holocene · Kunlun Mountains · Tarim Basin

T. Zihua (✉)
Key Laboratory of Cenozoic Geology and Environment,
Institute of Geology and Geophysics,
Chinese Academy of Sciences, P.O. Box 9825,
100029 Beijing, People's Republic of China
e-mail: tangzihua@mail.iggcas.ac.cn

T. Zihua · M. Guijin
Xinjiang Institute of Ecology and Geography,
Chinese Academy of Sciences, 830011 Urumqi, China

C. Dongmei
Academy of Exploration and Development,
Northwest Company, SINOPEC, 830011 Urumqi, China

Introduction

Climate evolution history in the Tarim Basin, an extremely arid area, NW China, during the Holocene has drawn much attention in the last two decades. Concerning palaeoclimate, palaeoecolgy and palaeohydrology of the Tarim Basin, many results have been published with little consensus in between, and palaeoclimate processes varied from author to author (e.g., Chen et al. 2006, 2008; Feng et al. 1999, 2006; Jin et al. 1994; Mischke and Wünnemann 2006; Wünnemann et al. 2003, 2006; Yang et al. 2002; Zhao et al. 2008a; Zhong et al. 2004, 2007; Zu et al. 2003). Even based on the same indicators, such as pollen, sediment grain size and calcium carbonate contents, two research groups had broken Holocene records from the Tarim River valley (Feng et al. 1999) and the interior of the Tarim Basin (Jin et al. 1994) into similar chronological segments, but proposed totally different environmental processes. In general, lacustrine/fluvial deposits from arid areas keep polyphase processes or provenances, and integrated palaeoenvironmental signals at their relevant time scales: the water balance among evaporation, precipitation and runoff mainly from melt-water, the influxes of eolian and fluvial sediments, and the human impacts on regional vegetation and on lake sedimental processes. It is hard to separate regional or local signals from the complexities accurately, and further decipher their driving factors. Details about Holocene palaeoenvironment in the Tarim Basin thus remain vague although the observations accumulated.

The previous studies on environmental history during Holocene in the Tarim Basin are known mainly from isolated outcrops and indirect proxies from lacustrine sediment cores, whereas eolian loess on the Kunlun Mountains is ignored improperly. Comparing to lacustrine

sediments, loess is easier to sample, more reliable environmental implications because of its clear transporting and depositing processes, and more credible radiocarbon age for free from old carbon contamination. Quaternary loess of predominantly eolian origin blankets much of the northern slope of the Kunlun Mountains (Yang et al. 2002) (Fig. 1), which deposits under a drier background than the Loess Plateau since at least 880 kyr (Fang et al. 2002). The thickest eolian loess distributes on the northern slope between Hotan-Yutan south (on northern slope of Kunlun Mountains from 2500 to 4900 m a.s.l.) with the coarsest particle (mostly coarse silts and fine sands) (Liu 1965; Yang 2000). Taklimakan Desert is characterized by longitudinal ridges with complex barchan dunes and is moving obviously southwards (Xinjiang Comprehensive Exploration Team and Academica Sinica 1978; Zhu et al. 1988).

The distributive patterns of the loess and desert dunes indicate two major wind directions in this region, the NW winds and the NE and NEE winds. The former is the westerlies over from Pamir, and the latter are derived from the westerlies after passing through the East Tianshan Mountains, which finally form an east jet at lower level. These two currents, commonly carrying dust, converge at the lower reaches of the Keriya River and form strong convergent up-rising flow along the northern slope of the Kunlun Mountains (Li 2002), lifting fine dusts up to higher levels and then depositing, or being carried away by westerly jet at higher level. This process occurs all the year with an annual mean of floating dust days more than 150 days, up to 230 days.

In this paper, we present pollen and grain size results from a loess section on the northern slope of the Kunlun Mountains, a continuous, well-preserved record of environmental changes of the basin/desert from synchronous deposits of the desert, to reconstruct the palaeoclimate history of the latest 5 ka.

Materials and methods

The study section, KMA, locates at 2,850 m a.s.l. on the third terrace of the Keriya River along a fresh outcrop (Fig. 1). At a depth of 20 cm, the section can be divided into two portions. The upper consisting mainly of top-soils with rich organic matters and bio-holes, and the lower consisting of massive brownish-yellow loess. As a consequence of altitudinal and climatic contrasts, type of natural vegetation around the section is mountain desert grassland consisting dominantly of *Ephedra*, *Artemisia*, *Ceratoides*, *Festuca* and *Zygophyllum* (Wu 1995). There are hulless

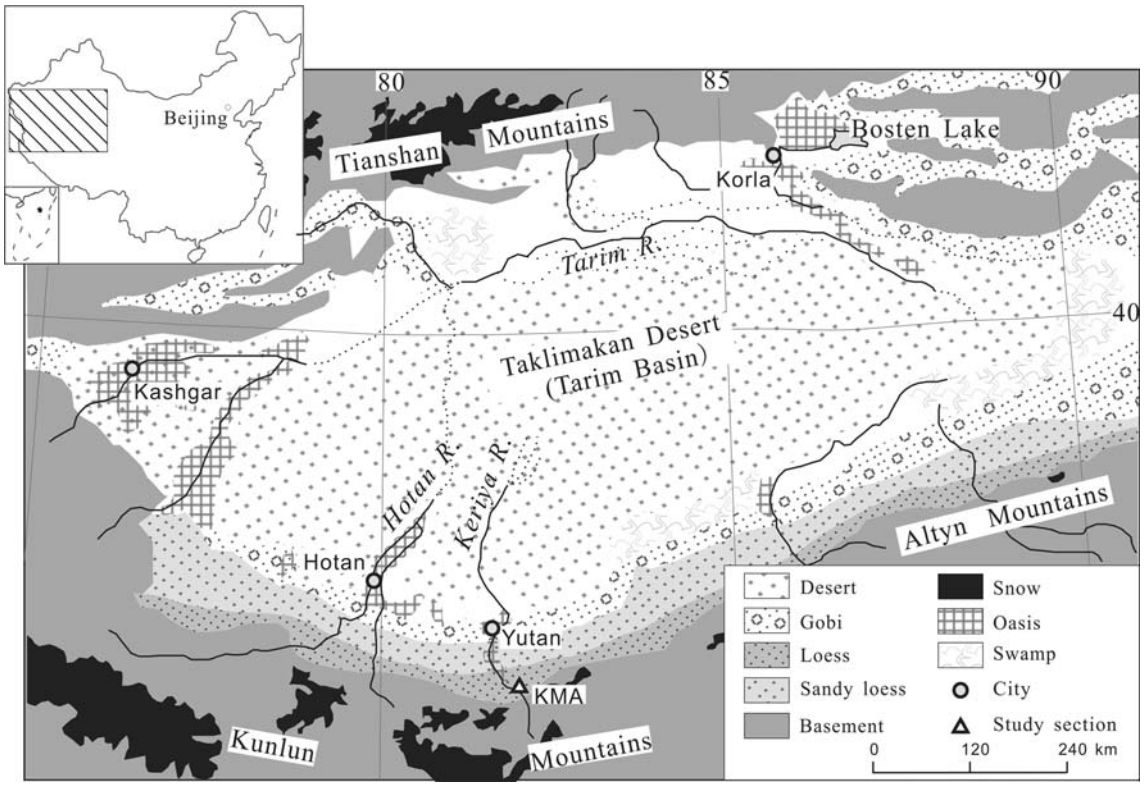

Fig. 1 Location map showing KMA section site (36°14.692′ N, 81°43.043′ E) and distribution of eolian facies in the Tarim Basin (redrawn from Zheng et al. 2003)

barley (*Hordeum*) and spring wheat (*Triticum*) as cultivated crops, with *Populus* planted along roads.

The section spans 492 cm in depth. Bulk samples (weight ca. 200 g each) for grain size and carbonate content were collected in 2 cm intervals at the upper part while the lower part below 124 cm depth in 5 cm intervals, yielding a total of 135 samples. After removal of calcium carbonate and organic matter, the chemical dispersant hexa-sodium metaphosphate $(NaPO_3)_6$ as well as the ultrasonic machine were employed to completely disperse the grain size samples (Lu and An 1997; Lu et al. 2002) before the treated samples were measured with the laser particle sizer Malvern Matersizer 2000 in the Particle Size Laboratory of Xinjiang Institute of Ecology and Geography, Chinese Academy of Sciences. Grain size parameters were calculated in the geometric method of moments by GRADISTAT program (Blott and Pye 2001). Contents of total organic matters and carbonates were estimated twice by loss on ignition at 550 and 950°C for 2 h, respectively, (Dean 1974; Heiri et al. 2001) with absolute errors better than 1 dw%.

Radiocarbon dating samples, KMA-D1, KMA-D2, and KMA-D3 were sampled at the depth of 120–124, 328–332, and 445–447 cm, respectively. The dating data were obtained by liquid scintillation counting method in the Radiocarbon Dating Lab of Seismological Bureau of Xinjiang Uygur Autonomous Region. Radiocarbon ages were calculated using the Libby half-life of 5,568 years and calibrated to calendar year (cal yr BP) using Calib 5.0.1 (Stuiver and Reimer 1993; Stuiver et al. 2007) with the INTCAL04 (Reimer et al. 2004) reference curve, and calibrated radiocarbon ages are used throughout the paper.

The sampling interval for pollen analysis between the depth of 0–132 and 132–492 cm is 6 and 5 cm, respectively. Accordingly, 94 samples for pollen analysis were taken and the temporal resolution can reach ca. 40–60 years per sample. The pollen samples were treated with acid-alkaline and heavy liquid flotation. The pollen grains were distinguished and counted under an optical microscope at a 400× magnification and the average counted grains was 127 grains with the maximum up to 265 and minimum 102. Pollen percentages were calculated based on a sum of all terrestrial pollen.

Results

A total of 26 pollen types were identified from the KMA section. On the diagram (Fig. 2), pollen spectra was drawn using the 10 most common taxa (>91% of the total pollen from each sample), and rare pollen that do not exceed abundance of 1% in any of the pollen spectra have been excluded from Fig. 2. *Ephedra* is the predominant pollen type in virtually all samples, comprising 16.2–70.9% (mean 51.9%) of the total pollen sum. Pollen of Chenopodiaceae (mean 12.0%), *Artemisia* (mean 7.3%), Compositae (mean 5.9%), *Ranunculus* (mean 5.0%) and Gramineae (mean 3.4%) is also common. Arboreal pollen (including *Picea, Alnus, Betula, Ulmus, Populus* and *Tilia*) is a minor component of the pollen record, average 1.9% per sample with exception between the depths of 0–70 cm. *Artemisia*/Chenopodiaceae (A/C) ratio, a moisture indicator due to the former pollen increases and the latter decreases with decreasing aridity (El-Moslimany 1990), fluctuate ranging from 0.02 to 1.8 with mean of 0.82. Two plateaus whose A/C ratio is not less than 1 occur at the depth of 160–190 and 265–300 cm, respectively.

Mean grain size (Mz) and sand content ($P_{>63\mu m}$) data derived from bulk samples display large and abrupt shifts (Fig. 3). Mz values vary from 32.5 to 54.5 μm and $P_{>63\mu m}$ values from 26.25 to 33.78%. The trends of Mz are mostly parallel to the $P_{>63\mu m}$ curve, displaying a noticeable correspondence between them. Furthermore, the Mz and A/C curves follow a similar pattern between 295 and 392 cm with high correlation 0.83, and for the whole record the correlation is relatively significant (correlation coefficient $r = 0.51$).

Carbonate content, as shown in Fig. 3, shows some major variations and robust increasing trends in the lower part 390–492 cm, but commonly remains a higher level of more than 10% with a slight increase up the section. In contrast, from the section bottom to the depth of 265 cm total organic materials (TOM) decrease from ∼0.32% to the minimum 0.16% with several brief excursions, and followed by a week increasing trend punctuated by three long-term fluctuations in the upward section.

The chronology is established by linear interpolation and extrapolation between radiocarbon results (Fig. 2) to assign age to each sample. The base age of the section is about 4900 cal years old and a mean sediment accumulation rate of 1.03 mm year^{-1} was determined. Clearly, the applicable estimation of consistent sediment accumulation rate may be questioned, particularly to the topsoil and the depth of 300–265 cm where coarser grain size could alter sediment accumulation rates. In spite of these limitations, the calculated ages used in the following provided the best chronology possible at this time.

Interpretation and palaeoenvironment reconstruction

Loess deposits are transported by wind from the proximal deserts, and their grain sizes are thus dominantly associated with the extent of the deserts and wind intensity. Theoretically, studies of Pye and his colleague (Pye 1987, 1995; Tsoar and Pye 1987) show that impact of dust grain size on

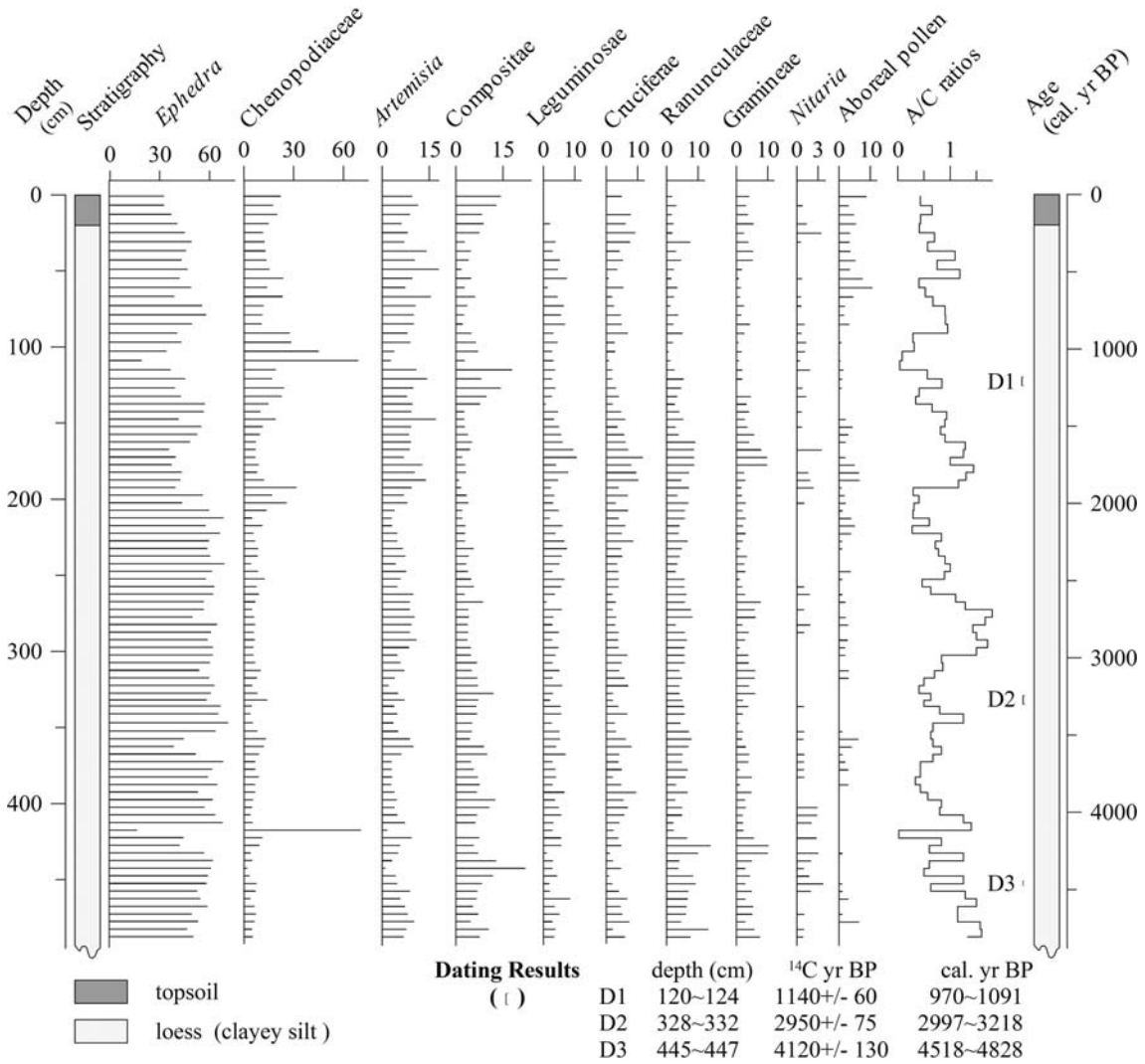

Fig. 2 Pollen percentage and A/C ratio of KMA section. Magnification is used to emphasize to changes in the percentages of the less abundant taxa

transport distance is notably greater than that of wind velocity. The maximum transported distance of a dust particle is inversely proportional to the fourth power of its grain size, while directly to the wind velocity. Field observation from Chinese Loess Plateau (Ding et al. 1999, 2005; Yang and Ding 2008) and Alaska (Muhs et al. 2004) also validated a similar pattern: over a short downwind distance, sand content in loess abruptly decreases so that can not be explained by wind intensity, but attribute to source-to-sink distance of sand-sized particles. Furthermore, wind intensity has no significant variations during the past 5000 years in the context of glacial and interglacial cycles (e.g., Küster et al. 2006; Nagashima et al. 2007). For sand-sized particles are considerable components of KMA section (Fig. 3) and their content is dominantly controlled by the source-to-sink distance, sand content ($P_{>63\mu m}$) was employed as an indicator of distance to the Taklimakan desert margin. High values of sand contents in KMA section are preferred to indicate comparatively close to the southern margin of Taklimakan desert.

Conventional interpretation of pollen data is usually based on presences and abundances of the indicator taxa and on the pollen ratios. The A/C ratio (El-Moslimany 1990) has been widely applied as a moisture indicator to the pollen spectra from arid regions (e.g., Herzschuh et al. 2004; Sun et al. 1994; Zhao et al. 2008b) to reconstruct changes in the local precipitation in that *Artemisia* is an important steppe component whereas Chenopodiaceae characterizes the desert vegetation. Sun et al. (1994) and Yu et al. (1998) proposed that Chinese desert areas yield A/C values below 0.5, and steppe more than 1. Combined with other proxies such as Gramineae and TOM content, A/C ratio provides a possibility for reconstructing moisture condition of the highland on the Kunlun Mountains.

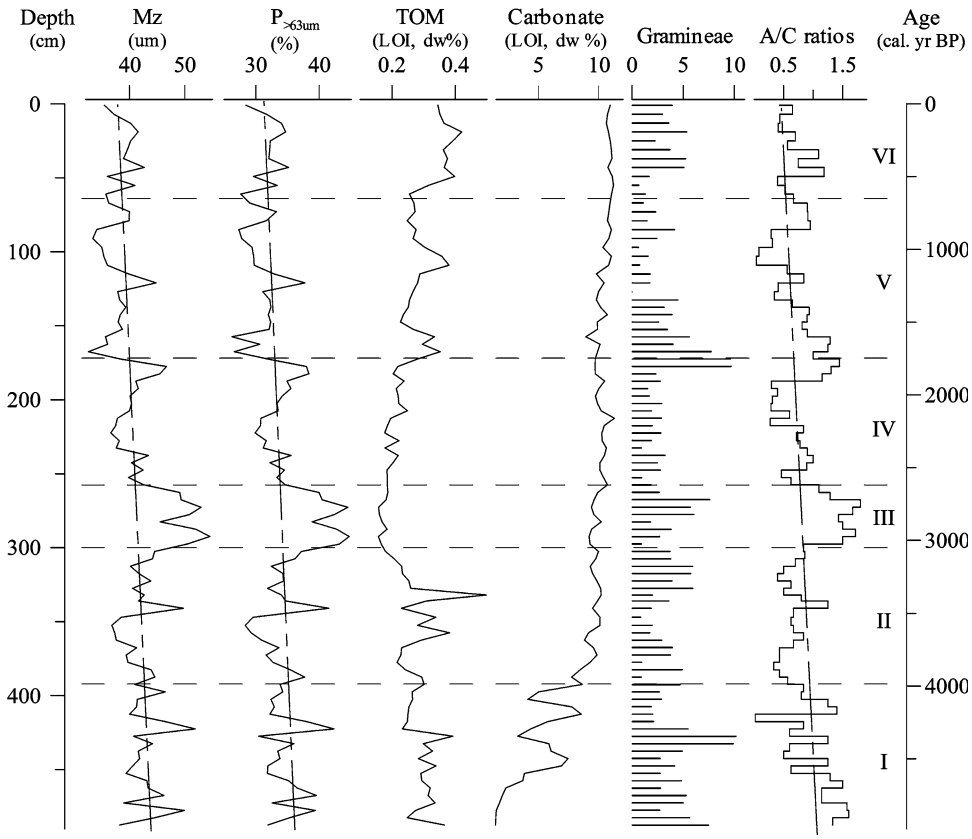

Fig. 3 Variations of the proxies (Mz, mean grain size; $P_{>63\mu m}$, sand content; TOM, total organic materials) and environmental stages named I–VI from result of constrained clustering of KMA section

If valid, the general climatic trends in both the south margin of the Tarim basin and the highland of Kunlun Mountains could be inferred from the proxies. The Mz and $P_{>63\mu m}$ records exhibit a gentle decrease with the exception of several brief periods of increase up the section, reflecting the Taklimakan Desert margin slightly retreat punctuated by transient, but significant advances during the past 5000 years. In contrast, the similar decrease in the A/C ratios up the KMA section indicates that moisture on the Kunlun highland lessened occurring over the same period. This long-term trends in the section locality toward drier conditions also expressed by a ~10% rise in carbonate content with most of the change occurring prior to 4000 cal yr BP. This most pronounced dry trend around 4000 cal yr BP probably be counterpart of the major enhanced aridity following the wet mid-Holocene in west part of Chinese Loess Plateau (Feng et al. 2004), in the Inner Mongolia Plateau except in the deserts (An et al. 2006), and even in arid central Asia (Chen et al. 2008).

The detailed environmental subdivisions named stage I–VI from bottom to top (Fig. 3) in the KMA section were established on the base of the proxies in Fig. 3 by the means of stratigraphically constrained clustering using the DPS program (Tang and Feng 2006).

Stage I (492–395 cm, ca. 4900–3950 cal yr BP). During this interval proxies of KMA section are primarily characterized by temporal and high-amplitude variations. Before ~3950 cal yr BP, although with sharp fluctuations, A/C slightly higher than mean value of entire section shows relatively more precipitation occurred at section locality. This wet condition is supported by relative higher TOM content and Gramineae in pollen spectra, as well as lower carbonate content. It is estimated from carbonization layers and snail horizons in sand-loess deposits by Wen and Qiao (1992) that temperature was 1°C higher and precipitation 50–100 mm more than presently ones from a highland in western Kunlun Mountains at ~4550 ± 230 yr BP (uncablirated age). However, the Mz which stayed at higher values and punctuated by abruptly increases suggested high intensity of sand drift activity in Taklimakan desert and shift southward of the desert. This interpretation is held out by the increasing sand content. As it is mainly transported by wind in saltation, higher sand contents indicated a shorter distance from the section to the southern margin of the desert. This unstable period may be a transition from the Holocene Optimum to late Holocene in this region.

Stage II (395–300 cm, ca. 3950–3050 cal yr BP). Values of Mz, and sand content which fluctuate at the mean levels of entire section, indicate that the sand activity from ca. 3950–3050 cal yr BP was rather stable with a brief advance-retreat cycle of the desert margin. Similar patterns

are observed from the TOM and A/C curves: a steady background interrupted by a temporal excursion with higher TOM and A/C values suggesting a moisture shift in situ. These antagonizing interpretations from KMA records may be implying that two completely different conditions coexist between the southern margin of the Taklimakan desert and the KMA locality, a highland on the Kunlun Mountains.

Stage III (300–260 cm, ca. 3050–2600 cal yr BP). Maximum sand activity in southern margin of the Taklimakan desert is indicated by grain size parameters between ca. 3050 and 2600 cal yr BP, and coincident increases in A/C ratios and Gramineae pollen suggest that the local climate became wetter. This event is in good agreement with the pervasive records in central Asia which correlate with Holocene Event 2 in North Atlantic (Bond et al. 1997), such as an abruptly increased climatic aridity at 3100 yr BP on the southern Loess Plateau (Huang et al. 2002), desiccation of Eastern Juyanze Lake between 3.2 and 2.9 cal kyr BP (Mischke et al. 2003), and an abrupt shift from warm-dry to cool-wet climate recorded in Gun Nuur, northern Mongolia (Wang et al. 2004). Mz and sand content are the highest in the section that display an expansion maximum of the Taklimakan desert and reflects the closest proximity from the section to the desert. At the section locality, as a contrast to the southern margin of the desert, A/C ratios are remarkably high and point to a long-lasting humid intervals. Different from the two previous periods, TOM reaching its minimum level does not show similar pattern to the fluctuations of A/C ratios and Gramineae pollen percentage. One reason for this could be that blooms of sand activity existed in the desert margin resulted in high accumulation rates of eolian dust in the section and diluted the coeval Gramineae pollen sedimentations during this period.

Stage IV (260–175 cm, ca. 2600–1750 cal yr BP). In general, during the period the KMA section area is under a stepwise drying condition indicated by decreasing A/C ratios and lower percentage of Gramineae pollen, and correspondingly in the southern margin of Taklimakan desert, the sand drift activity was restrained as shown on comparably stable Mz value and sand content. Only before this interval terminated, about 1800 cal yr BP, values of Mz, sand content, TOM and A/C ratios increased significantly, thereby indicating that sand drift activity of the desert recovered and effective moisture of the KMA section areas raised.

Stage V (175–64 cm, ca. 1750–640 cal yr BP). Except of carbonate content, all proxies during this period show comparatively low values and are punctuated by a positive excursion lasting from 1300 to 1200 cal yr BP. In terms of southern margin of the desert, lower values of grain size mean weaker sand drift activity, and the positive shift relate to relative robust sand drift activity. After 1200 cal yr BP, Mz and sand content curves almost reach the minimum and last for 100 years or more, meaning the desert retreat in this interval. And then, at about 900 cal yr BP the Mz and sand content curves restore to the level slightly lower than the section mean values. A/C ratios showing changes of moisture of the section locality confirm a similar change with the Mz, and thus display a palaeoclimatic process that antagonize ones existed in the southern margin of the desert: since about 1800 cal yr BP the KMA section locality was drying gradually and culminated around 1200 cal yr BP, and then approached to the entire section average level.

Stage VI (64–0 cm, 650 cal yr BP to present). This interval is corresponding temporally to the Little Ice Age. A typical introduced tree by recent human activity, *Populus* pollen appeared only above the depth of 62 cm, close to the base of this Stage. TOM contents above mean value and relatively higher Gramineae pollen percentages may support the interference of agricultural activities on sediments in KMA section locality. Thus, samples collected from top of the KMA section would be representative of the influence of anthropogenic activities, which may occasionally almost entirely mask the regional environmental information.

Discussion

Previous results showed a consistency of climatic changes between the southern margin of the desert and the highlands of Kunlun Mountains. What is more, some authors regarded the climatic records from the Guliya ice core located on the southern slope of Kunlun Mountains as a substitute of those of Xinjiang Region (e.g., Wang et al. 2001). For lack of a clear boundary of study area, the reconstructed palaeoclimate in the southern Tarim Basin would be overinterpreted, these conclusions or hypothesis, furthermore, are not supported by out data. As shown in Fig. 3 and mentioned above, the A/C ratio, which recorded moisture condition of the section locality, has positive correlation with mean grain size, a proxy of the intensity of sand drift activity in the southern desert. These observations suggest a crude simultaneity but opposition of environmental change between the section locality and the southern margin of the desert throughout the past 5000 years: an active time of sand drift in the southern margin of the Taklimakan Desert meets a wet time of the section locality; on the other hand, dry periods of the highland of Kunlun Mountains correspond to intervals of relatively stable sand activity in the desert margin.

Here a previously ignored question arises about linkages between the southern margin of the desert and the highland

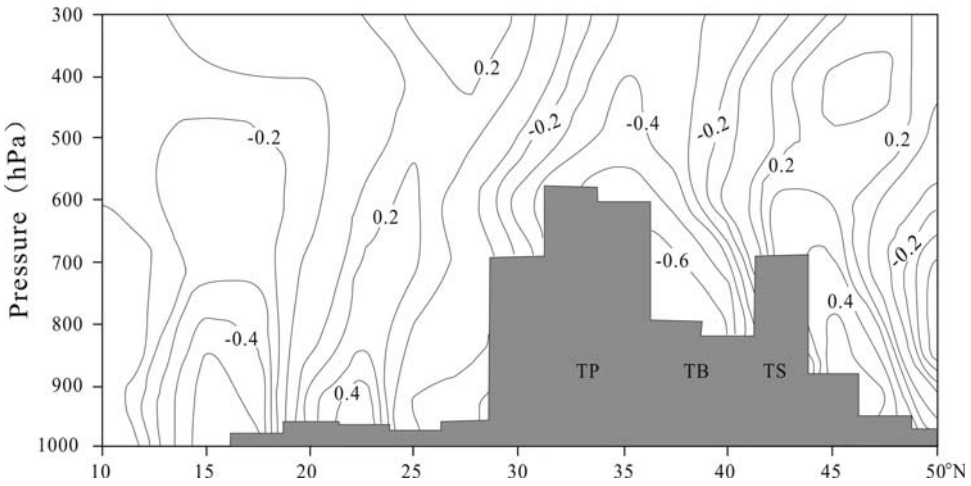

Fig. 4 Correlation coefficient between the summer precipitations in 82–82.5°E from 1958–2000 and the vertical velocity of 1000–300 hPa (*TP* Tibetan Plateau; *TB* Tarim Basin; *TS* Tianshan Mountains) (Modified from Feng et al. 2005)

on the Kunlun Mountains. The importance of the answer to the question not only lies in understanding of and better predicting trends of environmental changes in the Tarim Basin, also may improve the knowledge about the dynamics of moisture distribution vertically between the southern margin of the basin and the Kunlun highland. Recently, an opposite relationship between moisture at low and high elevations of the southern slope of Qilian Mountains (Zhao et al. 2008b) is reported and is interpreted as results of the interactions between subsiding air flow and monsoon-induced precipitation into the Qaidam Basin: uplifting air in the surrounding Qilian Mountains causes the air subsidence to extend into the Qaidam Basin. Different from the Qilian Mountains and Qaidam Basin, the central Tarim Basin is independent of East Asia summer monsoon system. So, the mechanisms for our study area need re-analyses.

Modern meteorological data may help to answer the question. Feng et al. (2005) discussed the correlation between summer precipitation and vertical velocity of 1000–300 hPa in 80°–82.5°E from 1958–2000 (Fig. 4) based on the NCEP/NCAR reanalysis data (Kistler et al. 2001). The obtained results could be available for reference in answering our question: the correlation coefficients of southern Tarim Basin and the northern slope of Kunlun Mountains are over or slightly less than 0.6 (Fig. 4) with a confidential level of 0.001. As to the KMA section area, when the dry air of NE and NW winds converge at the lower reaches of the Keriya River, they are too dry to form rain; later, they move southward and recharge moisture from the relatively wet mountains, and thus clouds and rain, often heavy, occur when they are severely forced to rise over the Kunlun Mountain range. In consequence, moisture difference exist between the southern margin and the highland of Kunlun Mountains, and enlarge when stronger winds occurred in the southern basin: stronger winds bring stronger ascending air in highland leading to heavier rains. The former result in coarser particle deposited in KMA section and the latter relate to the higher A/C value.

Concluding remarks

A decades-resolution time series since ~5000 cal yr BP is established for a loess section KMA from Kunlun Mountains based primarily on grain size parameters and pollen data. It provides a chance for plowing further details and causes of Holocene environmental history in Tarim Basin. Significant increase in carbonate content in KMA section implies a remarkable drying transition around 3900 yr BP in the section locality, and from then on, this dry condition remains as a background with minor wet oscillations. A high correlation between mean grain size and A/C ratio of pollen suggests a previously unrecognized pattern of moisture: the wet intervals in highland of Kunlun Mountains correspond to relative dry periods in southern margin of Tarim Basin. This moisture pattern would be results of the vertical variations of regional precipitation from the basin to the section locality.

Acknowledgments This work was supported by the Major State Basic Research Development Program of China (Grant 1999043502). We are indebted to anonymous reviewer(s) for valuable comments and suggestions to improve the manuscript. We also thank Wu Xinhua, Yan Shun, Yang Shiling, and Ali Aysa for helpful discussions, and An Jutian, Matkasm, and Azis for field assistance.

References

An CB, Feng ZD, Barton L (2006) Dry or humid? Mid-Holocene humidity changes in arid and semi-arid China. Quat Sci Rev 25:351–361

Blott SJ, Pye K (2001) GRADISTAT: a grain size distribution and statistics package for the analysis of unconsolidated sediments. Earth Surf Proc Land 26(11):1237–1248

Bond G, Showers W, Cheseby M, Lotti R, Almasi P, Priore P, Cullen H, Hajdas I, Bonani G (1997) A pervasive millennial-scale cycle in north Atlantic Holocene and glacial climates. Science 278(5341):1257–1266

Chen F, Huang X, Zhang J, Holmes JA, Chen J (2006) Humid Little Ice Age in arid central Asia documented by Bosten Lake, Xinjiang, China. Sci China Ser D 49(12):1280–1290

Chen F, Yu Z, Yang M, Ito E, Wang S, Madsen DB, Huang X, Zhao Y, Sato T, John B, Birks H, Boomer I, Chen J, An C, Wünnemann B (2008) Holocene moisture evolution in arid central Asia and its out-of-phase relationship with Asian monsoon history. Quat Sci Rev 27(3–4):351–364

Dean WE (1974) Determination of carbonate and organic matter in calcareous sediments and sedimentary rocks by loss on ignition: comparison with other methods. J Sediment Petrol 44(1):242–248

Ding Z, Sun J, Rutter NW, Rokosh D, Liu T (1999) Changes in sand content of loess deposits along a north-south transect of the Chinese Loess Plateau and the implications for desert variations. Quat Res 52(1):56–62

Ding ZL, Derbyshire E, Yang SL, Sun JM, Liu TS (2005) Stepwise expansion of desert environment across northern China in the past 3.5 Ma and implications for monsoon evolution. Earth Planet Sci Lett 237:45–55

El-Moslimany AP (1990) Ecological significance of common nonarboreal pollen: examples from drylands of the Middle East. Rev Palaeobot Palyno 64(1–4):343–350

Fang X, Lu L, Yang S, Li J, An Z, Jiang P, Chen X (2002) Loess in Kunlun Mountains and its implications on desert development and Tibetan Plateau uplift in west China. Sci China Ser D 45(4):289–299

Feng Q, Su ZZ, Jin HJ (1999) Desert evolution and climate changes in the Tarim River Basin during the past 12 ka. Sci China Ser D 29:87–96 (in Chinese)

Feng S, Zhang Y, Zhu D, Tang M, Gao X (2005) Guliya ice core accumulation and dry and wet change in south part of South Xinjiang Basin in the past 2000 years. Sci Geogr Sin 25(2):221–225 [in Chinese]

Feng ZD, An CB, Tang LY, Jull AJT (2004) Stratigraphic evidence of a Megahumid climate between 10, 000 and 4000 years BP in the western part of the Chinese Loess Plateau. Global Planet Change 43:145–155

Feng ZD, An CB, Wang HB (2006) Holocene climatic and environmental changes in the arid and semi-arid areas of China: a review. Holocene 16(1):1–12

Heiri O, Lotter AF, Lemcke G (2001) Loss on ignition as a method for estimating organic and carbonate content in sediments: reproducibility and comparability of results. J Paleolimn 25(1):101–110

Herzschuh U, Tarasov P, Wünnemann B, Hartmann K (2004) Holocene vegetation and climate of the Alashan Plateau, NW China, reconstructed from pollen data. Palaeogeogr Palaeoclimato Palaeoecol 211(1–2):1–17

Huang C, Pang J, Pinghua L (2002) Abruptly increased climatic aridity and its social impact on the Loess Plateau of China at 3100 BP. J Arid Environ 3:1–13

Jin H, Dong G, Jin J, Li B, Shao Y (1994) Environmental and climatic changes in the interior of Taklimakan desert since late glacial age. J Desert Res 14(3):31–37 (in Chinese)

Küster Y, Hetzel R, Krbetschek M, Tao M (2006) Holocene loess sedimentation along the Qilian Shan (China): significance for understanding the processes and timing of loess deposition. Quat Sci Rev 25(1–2):114–125

Kistler R, Kalnay E, Collins W, Saha S, White G, Woollen J, Chelliah M, Ebisuzaki W, Kanamitsu M, Kousky V (2001) The NCEP-NCAR 50-year reanalysis: monthly means CD-ROM and documentation. Bull Am Meteorol Soc 82(2):247–267

Li J (2002) Desert climate. China Meteorological Press, Beijing

Liu TS (1965) The Loess deposits in China. Science Press, Beijing

Lu HY, An ZS (1997) Pretreatment methods in loess-palaeosol granulometry. Chin Sci Bull 42:237–240

Lu HY, Miao X, Sun Y (2002) Pretreatment methods and their influences on grain-size measurement of aeolian "red clay" in north China. Mar Geol Quat Geol 22(3):129–135 (in Chinese)

Mischke CS, Demske D, Schudack ME (2003) Hydrologic and climatic implications of a multidisciplicary study of the mid to late Holocene Lake Eastern Juyanze. Chin Sci Bull 48(14):1411–1417

Mischke S, Wünnemann B (2006) The Holocene salinity history of Bostern Lake (Xinjiang, China) inferred from ostracod species assemblages and shell chemistry: possible palaeoclimate implications. Quat Int 154–155:100–112

Muhs DR, McGeehin JP, Beann J, Fisher E (2004) Holocene loess deposition and soil formation as competing processes, Matanuska Valley, southern Alaska. Quat Res 61(3):265–276

Nagashima K, Tada R, Matsui H, Irino T, Tani A, Toyoda S (2007) Orbital-and millennial-scale variations in Asian dust transport path to the Japan Sea. Palaeogeogr Palaeoclimato Palaeoecol 247(1–2):144–161

Pye K (1987) Aeolian dust and dust deposits. Academic Press, London

Pye K (1995) The nature, origin and accumulation of loess. Quat Sci Rev 14(7–8):653–667

Reimer PJ, Baillie MGL, Bard E, Bayliss A, Beck JW, Bertrand CJH, Blackwell PG, Buck CE, Burr GS, Cutler KB (2004) IntCal04 terrestrial radiocarbon age calibration, 0–26 Cal Kyr BP. Radiocarbon 46(3):1029–1058

Stuiver M, Reimer PJ (1993) Extended ^{14}C data base and revised CALIB 3.0 ^{14}C age calibration program. Radiocarbon 35(1):215–230

Stuiver M, Reimer PJ, Reimer R (2007) CALIB Radiocarbon Calibration. http://calib.qub.ac.uk/calib. Accessed 8 Jan 2008

Sun X, Du N, Weng C, Lin R, Wei K (1994) Paleovegetation and paleoenvironment of Manasi Lake, Xinjiang, N·W. China during the last 14000 years. Quat Sci 14(3): 239–248 (in Chinese)

Tang Q, Feng M (2006) DPS data processing system. Science Press, Beijing

Tsoar H, Pye K (1987) Dust transport and the question of desert loess formation. Sedimentology 34(1):139–153

Wang S, Gong D, Zhu J (2001) Twentieth-century climatic warming in China in the context of the Holocene. Holocene 11(3):313–321

Wang W, Feng Z, Lee X, Zhang H, Ma Y, An C, Guo L (2004) Holocene abrupt climate shifts recorded in Gun Nuur lake core, northern Mongolia. Chin Sci Bull 49(5):520–526

Wen Q, Qiao Y (1992) Paleoclimate records of Holocene sediment in Xinjiang, China. In: Shi Y, Kong Z (eds) The climates and environments of Holocene megathermal in China. China Ocean Press, Beijing, pp 168–174 (in Chinese)

Wu ZY (ed) (1995) Vegetation of China. Science Press, Beijing, pp 956–1021 (in Chinese)

Wünnemann B, Chen F, Riedel F, Zhang C, Mischke CS, Chen G, Demske D, Ming J (2003) Holocene lake deposits of Bosten Lake, southern Xinjiang, China. Chin Sci Bull 48(14):1429–1432

Wünnemann B, Mischke S, Chen F (2006) A Holocene sedimentary record from Bosten Lake, China. Palaeogeogr Palaeoclimatol Palaeoecol 234(2–4):223–238

Xinjiang Comprehensive Exploration Team, Academica Sinica (1978) Geomorphology of Xinjiang. Science Press, Beijing (in Chinese)

Yang SL, Ding ZL (2008) Advance-retreat history of the East-Asian summer monsoon rainfall belt over northern China during the

last two glacial-interglacial cycles. Earth Planet Sci Lett 274: 499–510

Yang X (2000) Loess deposits in the surrounding mountains of Tarim Basin, Northwestern China. Arid Land Geogr 23(1):13–18 (in Chinese)

Yang X, Zhu Z, Jaekel D, Owen LA, Han J (2002) Late Quaternary palaeoenvironment change and landscape evolution along the Keriya River, Xinjiang, China. Quat Int 97:155–166

Yu G, Prentice IC, Harrison SP, Sun X (1998) Pollen-based biome reconstructions for China at 0 and 6000 years. J Biogeogr 25(6):1055–1069

Zhao Y, Yu Z, Chen F (2008a) Spatial and temporal patterns of Holocene vegetation and climate changes in arid and semi-arid China. Quat Int 10.1016/j.quaint.2007.12.002

Zhao Y, Yu Z, Chen F, Liu X, Ito E (2008b) Sensitive response of desert vegetation to moisture change based on a near-annual resolution pollen record from Gahai Lake in the Qaidam Basin, northwest China. Global Planet Change 62(1–2): 107–114

Zheng H, Powell CM, Butcher K, Caom J (2003) Late Neogene loess deposition in Southern Tarim Basin: tectonic and palaeoenvironmental implications. Tectonophysics 375:49–59

Zhong W, Wang W, Tashpolat T, Xiong H, Shu Q (2004) Possible solar forcing of climate variability in the past 4000 years inferred from a proxy record at the southern margin of Tarim Basin. Chin Sci Bull 49(11):1190–1195

Zhong W, Xue J, Shu Q, Wang L (2007) Climatic change during the last 4000 years in the southern Tarim Basin, Xinjiang, northwest China. J Quat Sci 22(7):659–665

Zhu Z, Lu J, Jiang W (1988) Study on formation and development of Aeolian and trend of environmental change at lower reach of the Keriya River, Taklimakan Desert. J Desert Res 8(2):1–10 (in Chinese)

Zu R, Gao Q, Qu J, Qiang M (2003) Environmental changes of oases at southern margin of Tarim Basin, China. Environ Geol 44(6):639–644